

Convergence and Stability Assessment of Newton–Kantorovich Reconstruction Algorithms for Microwave Tomography

Nadine Joachimowicz,* Jordi J. Mallorqui, *Member, IEEE*,
Jean-Charles Bolomey, and Antoni Broquetas, *Member, IEEE*

Abstract—For newly developed iterative Newton–Kantorovich reconstruction techniques, the quality of the final image depends on both experimental and model noise. Experimental noise is inherent to any experimental acquisition scheme, while model noise refers to the accuracy of the numerical model, used in the reconstruction process, to reproduce the experimental setup. This paper provides a systematic assessment of the major sources of experimental and model noise on the quality of the final image. This assessment is conducted from experimental data obtained with a microwave circular scanner operating at 2.33 GHz. Targets to be imaged include realistic biological structures, such as a human forearm, as well as calibrated samples for the sake of accuracy evaluation. The results provide a quantitative estimation of the effect of experimental factors, such as temperature of the immersion medium, frequency, signal-to-noise ratio, and various numerical parameters.

Index Terms—Experimental data, inverse scattering, microwave tomography, nonlinear reconstruction.

I. INTRODUCTION

UNTIL now, microwave imaging techniques for biomedical applications are much less developed than those based on ultrasounds, X rays, nuclear magnetic imaging, or even electrical impedance tomography. Besides the technological aspects, which have been now almost successfully addressed, one of the most significant reasons for such a situation results from the complexity of the interaction mechanisms between a microwave beam and high dielectric contrast biological structures. Standard spectral diffraction tomography (SDT) approaches have been shown to offer limited capabilities in terms of quantitative reconstructions of the complex dielectric constant [1]. However, for a few years, microwave tomography has known a very significant step with the development of new reconstruction algorithms providing serious expectations in obtaining quantitative images [2]–[6]. More

particularly, the ability to proceed with high dielectric contrast targets marked a sharp difference with previous standard SDT algorithms. While such spectral techniques provided only qualitative results, namely, the equivalent current distribution in the target, quantitative techniques aim to a reconstruction of the dielectric permittivity of the target delivered from the local field dependence involved in the equivalent current distribution. As is well known, the price to pay is to solve a nonlinear inverse problem, instead of a linear one, for which different iterative techniques have been successively developed. One of the first of them to be successfully used for biomedical applications is probably the Newton–Kantorovich (NK) technique, which aims to iteratively minimize the error between the measured field scattered by the target and the scattered field calculated from a numerical model [7]–[9]. This technique has yielded unexpected good results in processing experimental data [10]. Unexpected means, here, that dielectric contrast as high as about ten have been successfully retrieved, with a very reasonable number of iterations. Unexpected, also, because the reconstruction was performed from true experimental data initially devoted to a spectral processing technique which is less demanding in terms of signal-to-noise ratio (SNR).

Regardless of how extremely encouraging these first results have been, some basic theoretical problems still remain concerning the stability and the convergence of the reconstruction process, with possible traps in local minima. Consequently, a better understanding of the operational capabilities of iterative algorithms has stimulated 1) an extended assessment of the noise robustness, as well as 2) a systematic study of the impact of both experimental and model errors involved in NK tomographic reconstructions.

This paper is organized as follows. First, the experimental setup will be rapidly described, as well as the targets used for the stability assessments. The case of a human forearm will be used as an example of a complex biological structure. For error quantification purposes, a phantom consisting of plastic tubes with different liquid fillings of known dielectric constant will be systematically used. The second part will be devoted to the numerical techniques used for solving both the direct and the inverse scattering problems. The solver of the direct problem is based on an electric-field integral equation formulation, while the inverse problem is solved by means of NK technique. For the reader who is not a

Manuscript received August 7, 1997; revised January 8, 1998. The Associate Editor responsible for coordinating the review of this paper and recommending its publication was M. W. Vannier. *Asterisk indicates corresponding author.*

*N. Joachimowicz is with the Université Paris VII, Laboratoire des Signaux et Systèmes/Electromagnetics Department, Supélec, Plateau de Moulon, 91192 Gif-sur-Yvette, France (e-mail: joachimowicz@supelec.fr).

J. Mallorqui and A. Broquetas are with the Universitat Politècnica de Catalunya, Department of Signal Theory and Communications, Campus Nord UPC-D3, Barcelona, Spain.

J.-C. Bolomey is with the Université Paris XI, Laboratoire des Signaux et Systèmes/Electromagnetics Department, Supélec, 91192 Gif-sur-Yvette, France.

Publisher Item Identifier S 0278-0062(98)08047-1.

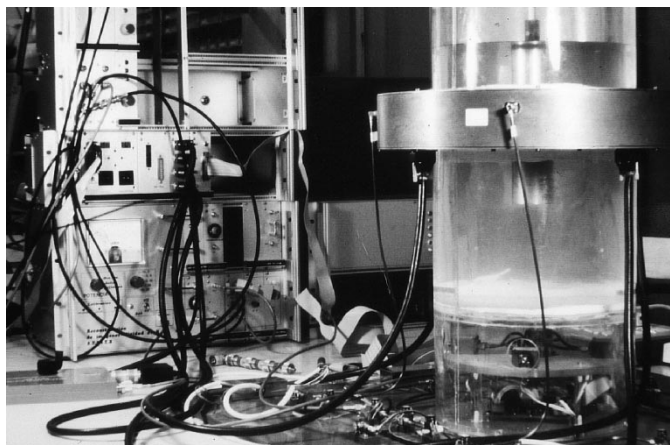


Fig. 1. Photograph of the 2.33-GHz circular scanner.

specialist of nonlinear inversion of scattering problems, it is worth explaining that NK technique has been shown to be equivalent [9], [17] to the so-called distorted Born method (DBM) developed independently, but almost simultaneously, by Chew [3]. Finally, the third part presents some representative results for illustrating the dependence of the reconstructed image on the most critical experimental and numerical parameters.

II. DESCRIPTION OF THE MICROWAVE SCANNER

The microwave scanner operating at 2.33 GHz, used for providing the experimental data (Fig. 1), has been extensively described in previous papers [11], [12]. It consists of a 25-cm-diameter circular array of 64 water-immersed horn antennas. The electric field is parallel to the array axis. The targets are introduced in a cylindrical water tank. Water immersion is used to reduce reflexion losses of high-water-content targets and minimizes external parasitic paths around the targets. Furthermore, it provides a significant improvement of the spatial resolution, via wavelength contraction, by a factor of the order of ten, due to the high dielectric constant of water [13]. Each of the array antennas can operate either in a transmitting or receiving mode. The measurement procedure records the scattered field values at the receiving antennas, when all the array antennas are successively used as transmitters. As a matter of fact, when one antenna is transmitting, the scattered field is measured only with the 33 antennas located in front. Consequently, at the end of the measurement procedure, the data file consists of $33 \times 64 = 2112$ complex values of the scattered field. The scattered field is deduced from the total measured field by subtracting the incident field, measured in the absence of any target. The selection of the measurement channel, as well as the switching between transmitting and receiving modes, is achieved via the modulated multiplexing technique [12]. A double modulation scheme has been used to solve one of the major problems encountered in developing the equipment, namely, interferences and crosstalk between the different transmitting and the receiving channels. In typical operational conditions, the SNR is around 20 dB.

As explained earlier, the biological target or the phantom is immersed in water. It is worth pointing out that the dielectric

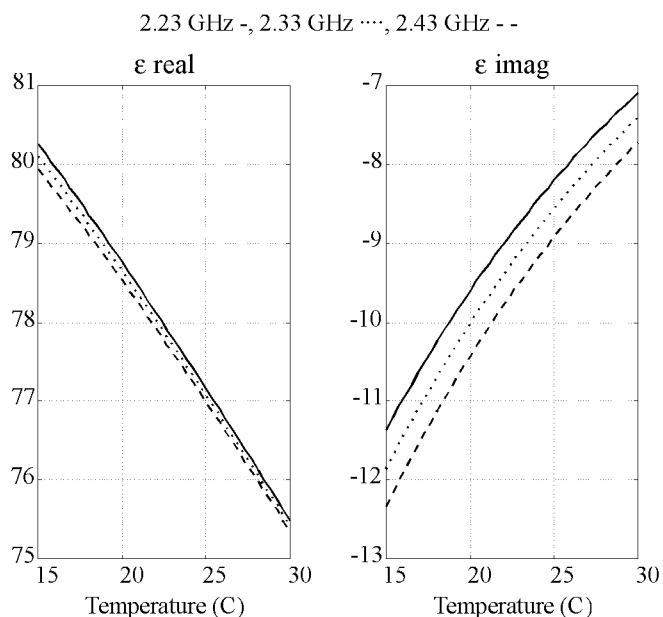


Fig. 2. Sensitivity of the dielectric constant with respect to frequency and temperature.

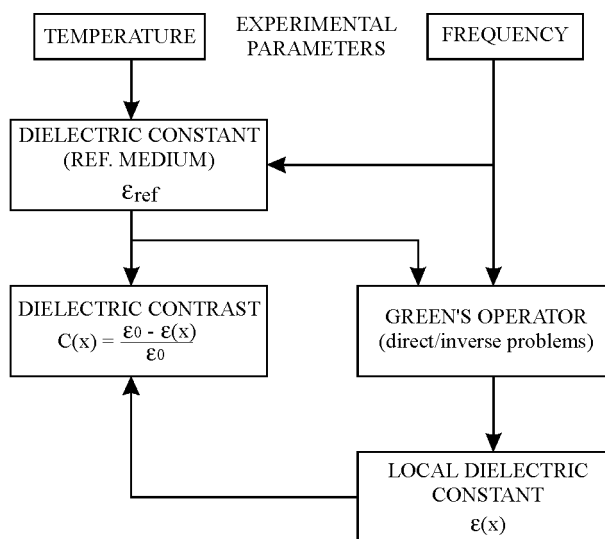
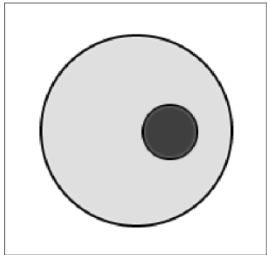


Fig. 3. Flow-chart for illustrating the impact of temperature and frequency on the reconstruction of the dielectric contrast in a biological target.

constant of water depends both on frequency and temperature. Concerning the frequency aspect, the microwave generator provides a short- and long-term stability less than 1 MHz. Temperature uniformity is expected to be maintained within ± 1 °C in the water tank. The temperature coefficient of the water dielectric constant is about $-0.5\%/^{\circ}\text{C}$ for the real part, and $+2\%/^{\circ}\text{C}$ for the imaginary part. Stogryn's model [14] has been used to obtain the sensitivity of the dielectric constant with respect to frequency and temperature (Fig. 2). It can be observed that temperature effects are significantly more sensitive than frequency effects within the previously indicated experimental margins for the water temperature, and the source stability in frequency. However, frequency also has a direct impact on the Green's operators which are involved in the tomographic reconstruction process. Fig. 3 shows a flow-chart

TABLE I
REAL AND IMAGINARY PARTS OF THE DIELECTRIC CONSTANT OF
THE DIFFERENT MEDIA INVOLVED IN THE REFERENCE TARGET



	ϵ_r'	ϵ_r''
water	77.3	8.66
4% ethylic alcohol	73	11
96% ethylic alcohol	10	8.3
plexiglass	2.73	0.01

explaining how both frequency and temperature uncertainties may influence the accuracy of the dielectric contrast retrieval.

Before any set of measurements, the array is calibrated for compensating unavoidable amplitude/phase dispersions in the response of its different elements. The calibration procedure is performed with a 4-cm-diameter metallic cylinder located at the center of the water tank. The knowledge of the field scattered by such a reference target allows to determine the weighting factors to be applied for the transmission coefficient between any pair of antennas. The targets to be considered in this paper are an human forearm, and a cylindrical phantom for which the dielectric constant has been measured. The first one is representative of a true complex biological structure, while the second is more convenient for quantitative assessment purposes. The real and imaginary parts of the dielectric constant of the cylindrical four-constituents phantom are given in Table I.

III. RECONSTRUCTION METHODS

The reconstruction of the permittivity image from the measured fields falls in the domain of the so-called inverse scattering problems, which exhibit some intrinsic difficulties. First, the propagation of electromagnetic waves in objects whose dimensions are a few wavelengths, cannot be modeled with ray tracing techniques. Strong diffraction effects have to be taken into account. Second, the scattered fields are only measured in a limited zone of space, basically on a finite part of the antenna array (the antenna domain), but not inside the target under test (the object domain). Third, due to the high dielectric contrast of biological tissues and their attenuation, the contribution of the inner part of the target to the scattered fields risks to be shadowed by the huge scattering of the external layers. Due to these effects, the inverse scattering problem for biological case is strongly nonlinear and ill-conditioned. Two different techniques have been investigated, the SDT and the spatial iterative NK approaches.

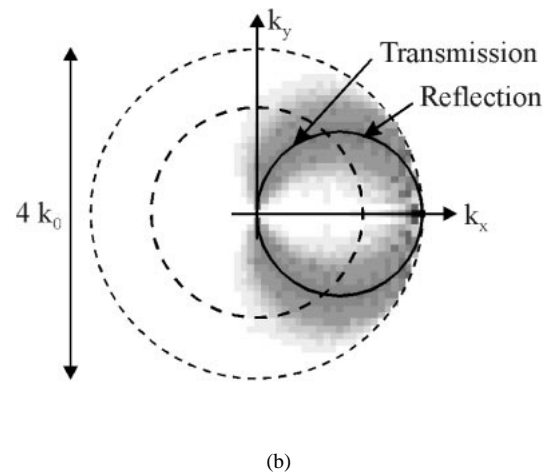
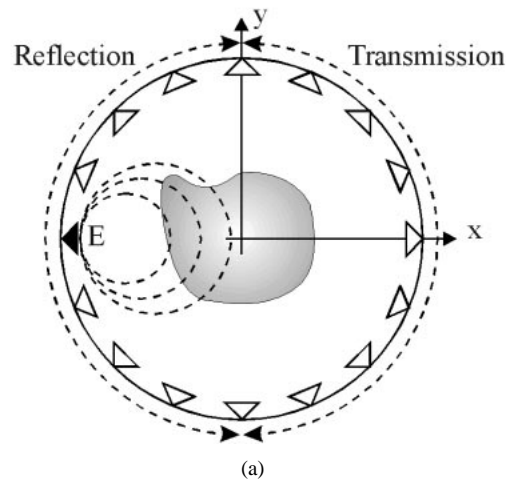


Fig. 4. (a) Reflection and transmission arrangements for microwave tomography and (b) filling of the contrast spectral plane in the case of a plane wave (solid line), or a cylindrical wave (shadowed zone).

A. Diffraction Tomography Algorithm

In this technique, the complex permittivity is determined from the computation of the induced current with Born's approximation, that assumes the body slightly perturbs the incident field. Under this hypothesis, the total field inside the body is approximated by the incident one, allowing the formulation of the inversion problem as a mapping of the field data on the image bidimensional spectrum [15]. For each emitter position, the scattered field is measured on the other elements of the array [Fig. 4(a)]. In the case of an incident plane wave, each set of measurements contributes to one circle over the contrast bidimensional spectrum of the object, as it is shown in solid line in Fig. 4(b). If the incidence is a cylindrical wave, the algorithm can be modified, and then each measurement set supplies information about a larger number of points on the contrast spectrum, that corresponds to the shadowed zone on the same figure. By changing the emitting antenna or the direction of the incident plane wave, the whole available spectrum is filled and the reconstructed contrast map can be obtained by means of an inverse fast Fourier transform (FFT). Due to the limitations on the accessible points of the contrast spectrum that can be

filled with measurements, the reconstructed object is a low-pass filtered version of the original one. Note that, here, only the transmission informations have been used.

Quasi-real-time images can be obtained with diffraction tomography, since FFT can be efficiently used. However, they present two major limitations. First, Born approximation assumes a weak scattering situation for approximating the total field in the scatterer by the incident one. Due to high contrast of biological bodies, causing multiple scattering, this approximation is not valid and the images obtained are only qualitative in the best case. Second, the loss of information contained in high spatial frequency components, especially in the invisible range, limits the spatial resolution to one-half of a wavelength in the immersion medium. A part of high spatial frequency components can be recovered by injecting some *a priori* information, such as the target contour, for instance [16]. However, diffraction tomography is not very suitable for efficiently introducing *a priori* information.

B. Newton–Kantorovich Algorithm

The limitations of the diffraction tomography approach have recently stimulated the development of new iterative techniques for obtaining quantitative reconstruction of highly contrasted objects due to a better use of the available *a priori* information. One of them is the NK technique. In a NK algorithm, a Newton-type iterative scheme is used to adjust an *a priori* contrast distribution by minimizing a cost function, which reflects the difference between the measured scattered field, and the simulated scattered field obtained from a numerical estimation. The NK algorithm can be decomposed in successive steps. First, a moment method with pulse basis function and point matching is used to generate matrix equations from the electrical field integral equation (EFIE). This step is equivalent to transform into a discrete form the nonlinear operator which relates the unknown dielectric contrast to the scattered field. Then, at each iteration, the nonlinear operator is linearly approximated around a current estimate of the contrast, by applying a Newton-type procedure. It has been shown [4], that, by considering small changes and only keeping first-order variations, an analytical expression of the derivative matrix is obtained. This leads, at each step, to a matrix relation between a small variation of the scattered field (the difference with respect to the data), and a small change of the contrast (the correction to update the current contrast). Extending the resulting former matrix relation to multiview configuration leads to an overdetermined system, which is solved for a least-squares solution.

The general iterative principle of the algorithm represented in Fig. 5 can be summarized as follows. For a set of incident beams, the field scattered by the object under test is measured. The measured data are then compared with the estimated data obtained by solving the direct scattering problem associated with a given object illuminated with the same interrogative beams. At the beginning, the object is described by using all the available *a priori* information. After comparing the measured and the estimated scattered fields, the object's dielectric constant is updated by inverting the derivative matrix. The

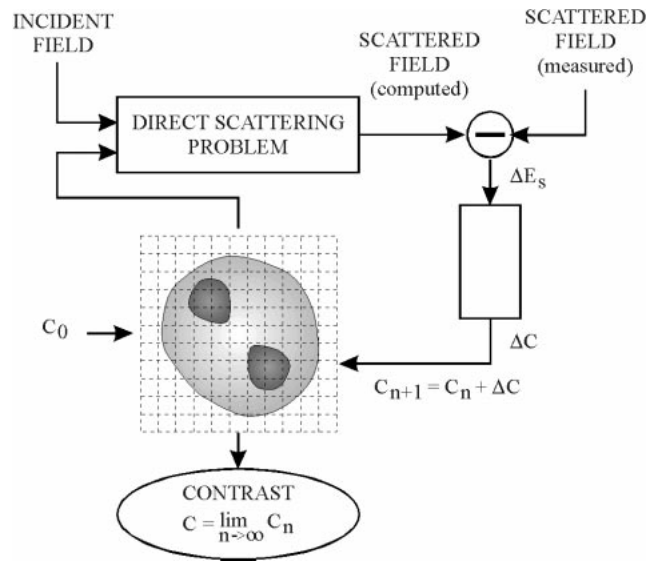


Fig. 5. Principle of the nonlinear reconstruction scheme.

inversion scheme used here depends on the method used to reach the regularization parameter. As a matter of fact, the numerical instability of the inverse scattering problem here is related to the large condition number of the linear least-squares problem. Hence, a Tikhonov regularization procedure is applied. It consists to reduce the condition number of the matrix to be inverted by increasing the weight of its diagonal elements, by introducing of a regularization parameter. Consequently, a strong value of this parameter stabilizes the inversion procedure, but may smooth the solution too much and, thus, decrease the spatial resolution. On the other hand, a low value of the regularization factor may affect the stability and the convergence of the iterative process. Therefore, one must look for a somewhat delicate compromise between fitting data and reducing the effect of noise amplification on the solution. Two strategies have been investigated for choosing the regularization parameter: an empirical method, which is detailed in [4], and a generalized cross-validation method (GCVT), which is a weighted version of ordinary cross validation [17]. GCVT is based on the minimization of a real function, depending on the singular value decomposition of the derivative matrix, and on the data. Hence, for a sake of conserving time, the linear least-squares problem is solved, in this case, with a singular value decomposition. The details of the GCVT algorithm used here, are developed in [18]. The result of these two strategies are shown in the Section IV).

IV. IMPACT OF NUMERICAL PARAMETERS

A. A Priori Information

The iterative aspect of the reconstruction easily allows the introduction of *a priori* information concerning the object. This *a priori* information has a significant impact on the convergence of the process. Indeed, information such as contour of the object, upper and lower bounds of the dielectric contrast, etc., reduces the class of the permittivity distribution

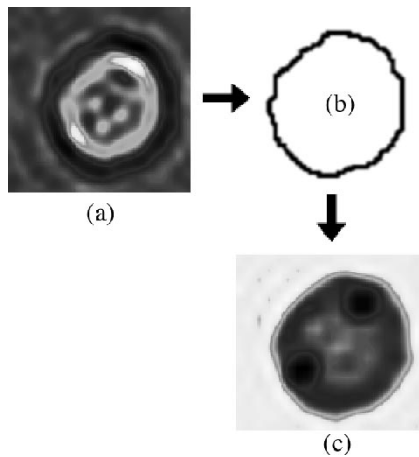


Fig. 6. Procedure for using the target contour provided by diffraction tomography reconstruction as *a priori* information for NK reconstruction (a) diffraction tomography, (b) contour extraction, and (c) NK.

to be retrieved and contributes to recover the rapidly varying components which are filtered out during the regularization process, to be further discussed later. However, too many constraints may provide bad results by greatly reducing the degree of freedom of the reconstruction procedure. In the case of unknown complex structures, it may be interesting to use the result of SDT process to introduce an approximate external contour of the target as *a priori* information. Indeed, SDT appears as a convenient technique for estimating the external contour because it can be operated under the same experimental conditions and does not require any additional measurement. The same data are processed. Therefore, this is the easiest procedure for supplying *a priori* information which take into account systematic errors as the positioning's object and sensors errors, for example. Fig. 6 shows how such a procedure works in the case of a human forearm. For simpler targets, such as reference cylindrical samples for which the external dimensions and the dielectric constant are known, different initial guesses can be considered for the sake of illustrating the effect on the reconstruction. Fig. 7 shows the results obtained for four different initial guesses. The first [Fig. 7(a)] corresponds to no *a priori* information at all, in that sense that the dielectric constant at the target location is chosen equal to water permittivity. The second [Fig. 7(b)] and the third [Fig. 7(c)] correspond, respectively, to the spatial averaged value, either for water and the target in the square reconstruction area or for the target only in the area effectively occupied by the target. Finally, in the fourth example, which provides the best final result, the initial guess has been determined empirically by selecting the image exhibiting the lowest residual error on the scattered field. As shown on Fig. 6, the reconstruction algorithm succeeds, in any case, in retrieving the correct shape and dimensions of both external and internal cylinders. However, the introduction of the external contour is necessary to obtain satisfactory quantitative results. Consequently, in the following, this *a priori* information will be systematically used. Practically, as explained earlier, this information could be rapidly derived from a preliminary SDT processing of the measured data.

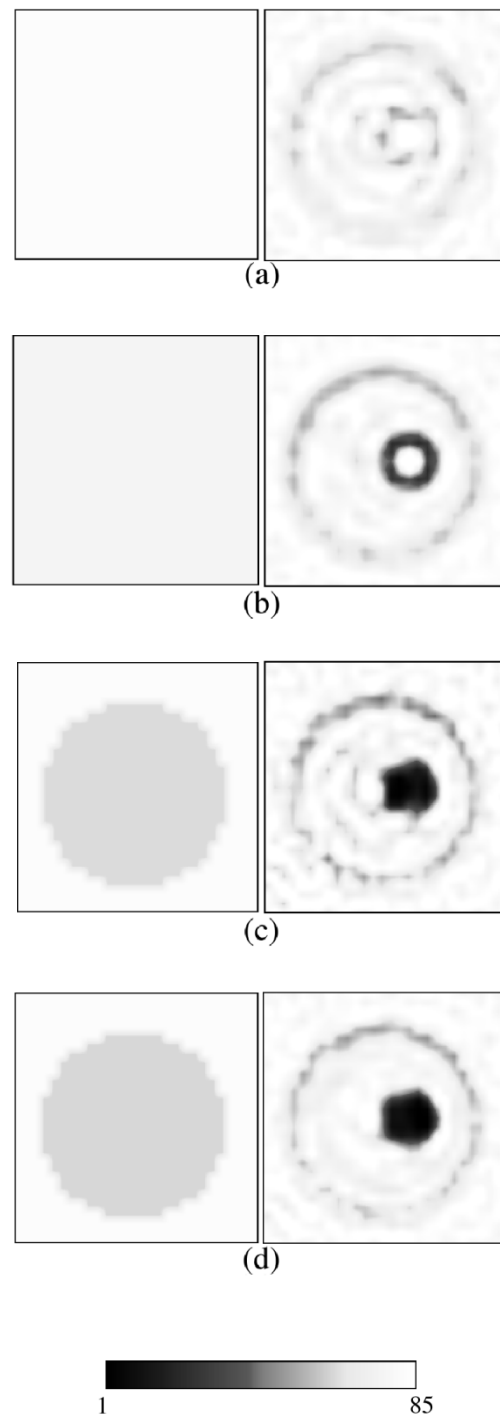


Fig. 7. Effect of dielectric contrast *a priori* information.

B. Discretization

The discretization effect in the NK technique has been assessed by considering a “fine” 0.1-wavelength mesh and a “coarse” 0.3-wavelength mesh. As shown in Fig. 8, the image human forearm quality is comparable for either the fine or the coarse mesh, as soon as experimental data are processed. This is mainly because the experimental data exhibit relatively low SNR's, about 20 dB in typical situations. The noise content in the scattered field shadows the information related to sharp

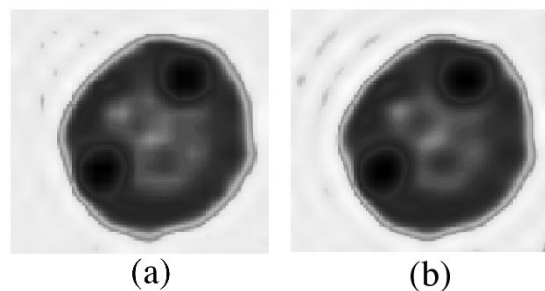


Fig. 8. Effect of the size of the discretization mesh (a) $\lambda/3$ and (b) $\lambda/10$.

details in the target. As it was observed with numerically simulated experimental data with higher SNR, the image quality is improved when the mesh size is reduced. However, reducing the mesh size results in higher computation times and memory size requirements. For instance in a CONVEX 3480 vectorial computer, in the human arm (the largest object reconstructed) four iterations require 1.5 h for a 0.3λ mesh size (19×19 complex unknowns) and 8 h for a 0.1λ mesh size (57×57 complex unknowns). Furthermore, a finer mesh requires a stronger regularization for ensuring the convergence of the iterative process. Despite the fact that the linear set of equations may be underdetermined in this case, the NK algorithm can converge due to the strong correlation between adjacent pixels resulting from the low-pass filtering effect of the scattered field [19].

C. Regularization Technique

In Section III-B, it was explained that a Tikhonov regularization technique is used to reduce ill conditioning and to improve convergence. Two distinct methods have been investigated for determining the regularization factor involved in such approaches. The first method is the so-called GCVT. In the second method, the regularization factor is determined empirically. As compared with this second method for which the regularization factor must be initially fixed, GCVT requires fewer arbitrary choices to be performed and operates more systematically at the different steps of the reconstruction process. However, despite its empirical aspect, the second method provides comparable accuracy for a wide range of values of the regularization factor. Consequently, it has been shown to lead more rapidly to good results, but less stable than with GCVT. Fig. 9 shows a typical example of reconstructions performed with these two techniques in the case of a cylindrical reference target. At the third iteration, the two methods provide comparable error on the scattered field and on the image. With GCVT, the fourth iteration is practically equal to the previous one, while with the empirical method it differs more significantly. The use of GCVT results in higher computation time because of SVD decomposition. Therefore, in the following, the empirical method will be systematically used.

V. IMPACT OF EXPERIMENTAL PARAMETERS

A. Signal-to-Noise Ratio

The assessment of the sensitivity of the image quality to the SNR has been performed as follows. Instead of changing it

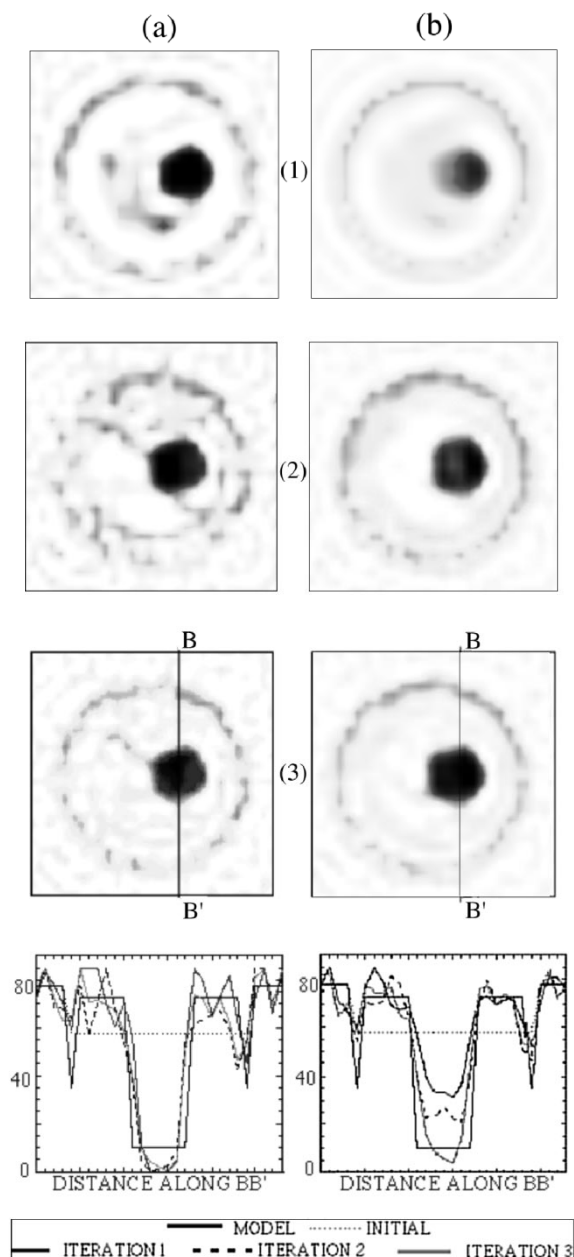


Fig. 9. Effect of the regularization technique during the iterative process. (a) Empirical and (b) GCVT.

experimentally, it appeared more convenient to use a numerical approach. Noiseless data have been synthesized numerically by solving the direct problem, via the integral equation. A white Gaussian noise has then been added to noiseless data for simulating noisy data with decreasing SNR's, namely 40 dB, 30 dB and 20 dB. As far as multiview measurements are performed, the SNR is defined from the maximum of the different projection maxima. For each of the previous SNR values, the tomographic images have been reconstructed and compared with the image corresponding to noiseless, infinite SNR, as shown in Fig. 10. Obviously, the image quality is decreasing with SNR. More particularly, it can be observed that the image obtained with 20-dB SNR is very comparable to the image deduced from experimental data. Such an overall

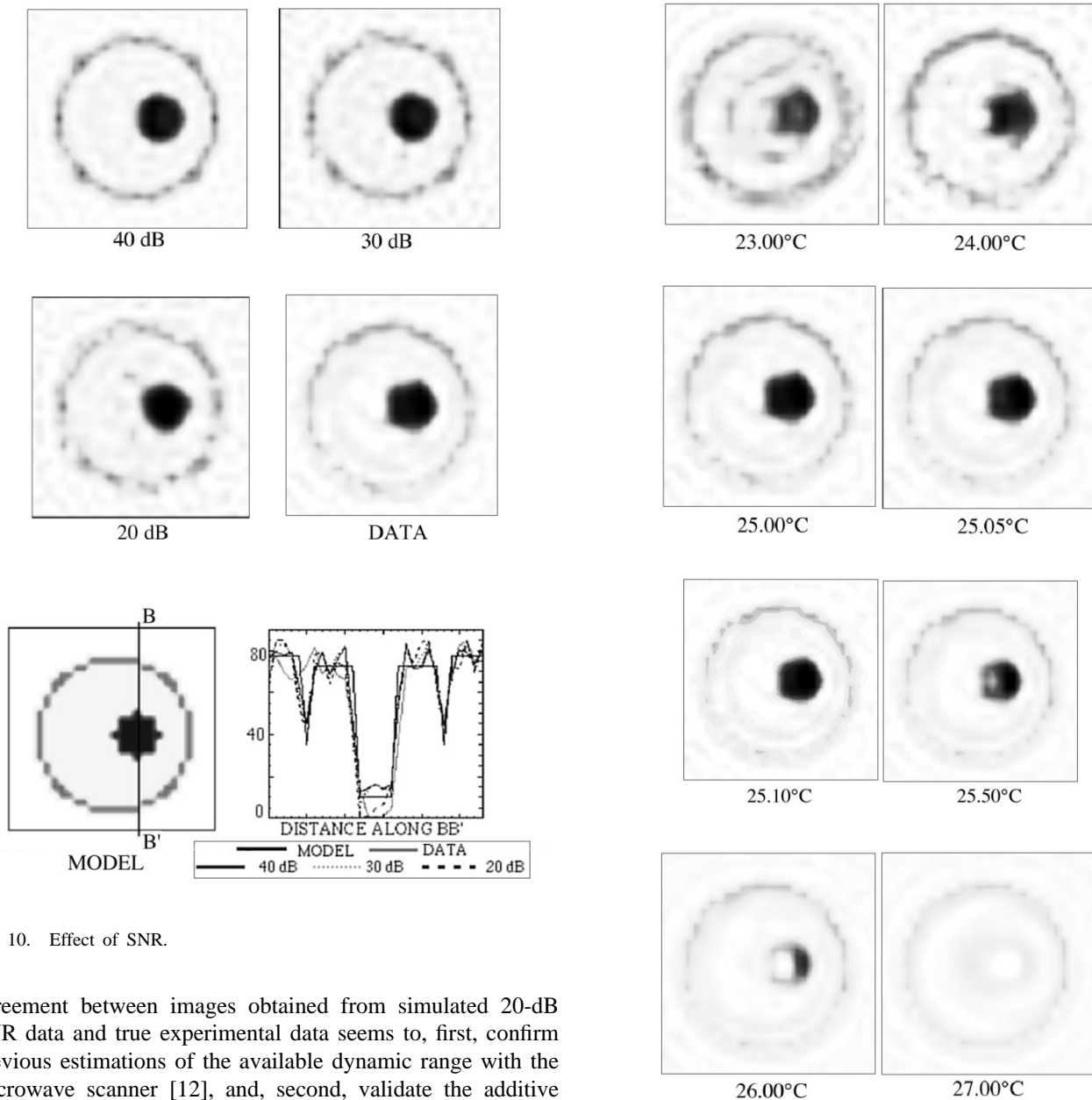


Fig. 10. Effect of SNR.

agreement between images obtained from simulated 20-dB SNR data and true experimental data seems to, first, confirm previous estimations of the available dynamic range with the microwave scanner [12], and, second, validate the additive Gaussian noise model for assessing the noise robustness of reconstruction algorithms.

B. External Medium

At 25 °C, measured in the scanner water tank, the relative dielectric constant of water is equal to 77.3 for the real part and 8.66, for the imaginary part. For determining the impact of the temperature on the final image, reconstructions have been performed with different values of the dielectric constant. The temperature has been increased from 23 °C up to 27 °C. The results can be seen on Fig. 11. It clearly appears that the temperature has a significant influence. The “best” image seems to be obtained at 25 °C, which was the temperature effectively measured in the water tank. Fig. 11 shows also the evolution of the error on the reconstructed image as a function of temperature: a marked minimum exists at 25 °C. A few tenths of a degree (°C) error in the temperature results in visible effects, via the dielectric

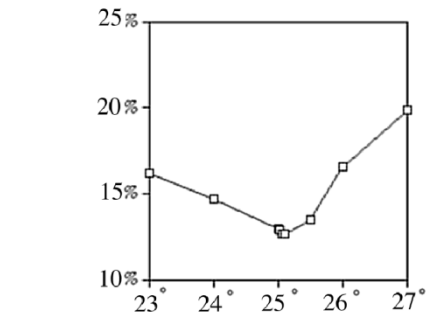


Fig. 11. Effect of the temperature of the immersion medium.

constant, on the reconstructed images. Some indicative value of the accuracy on the reconstructed dielectric constant can be deduced, assuming that the experimental temperature margin is of the order of ± 1 °C. The corresponding water-relative

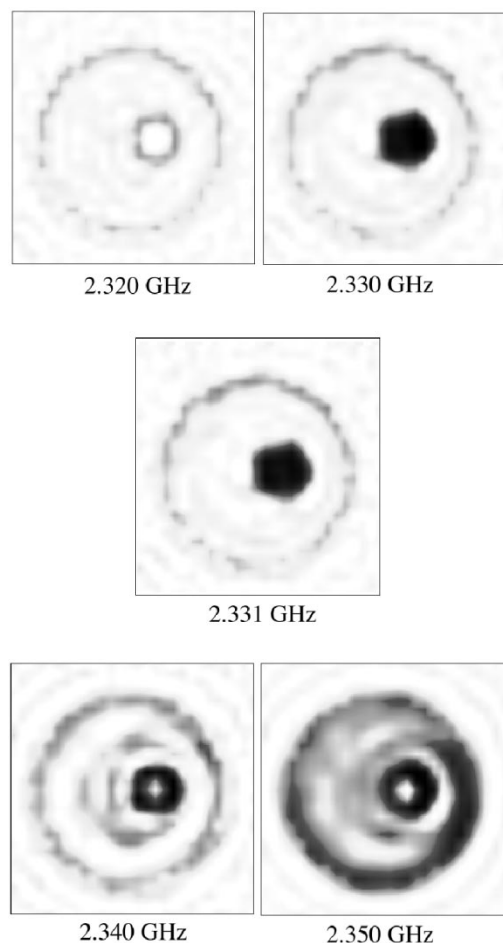


Fig. 12. Effect of the frequency.

uncertainty on the dielectric constant is about $\pm 1\%$. The significant effect of temperature can be explained by the high temperature dependence of water dielectric constant (Fig. 2).

C. Frequency

As explained earlier, the impact of the frequency on the dielectric constant can be reasonably neglected. On the contrary, its impact via the Green's operators [4] is clearly illustrated on Fig. 12, which shows the reconstructed images for frequencies varying between 2.230 GHz and 2.350 GHz. Here, again, the “best” image—which corresponds to a minimum of the reconstruction error—is obtained at the expected operating frequency of 2.330 GHz. Apart from this value, ± 1 MHz frequency deviation results in visible deteriorations of the reconstructed images.

VI. CONCLUSION

NK techniques (equivalently, DBM) provide a very significant improvement as compared with standard SDT. Consequently, they pave the way to an effective use of microwave tomography for biomedical and even industrial applications [20], [21]. Identified biomedical applications include functional imaging via dielectric characterization, noninvasive thermal sensing, and monitoring of inflammatory processes resulting,

for instance from accidental or therapeutic irradiation, as well as from rejection mechanisms after organ transplants. On the industrial side, multiphase flowmetry in vessels, fluidized beds, constitutes an objective of recognized practical relevance. For all these applications, microwaves are expected to provide adequate contrast with acceptable spatial resolution. However, the systematic studies which have been conducted on true experimental data, obtained from volunteers and phantoms, demonstrate the sensitivity of the NK technique with respect to various experimental and model errors. It is particularly worth mentioning that the effects of these errors have been comparably confirmed with two distinct reconstruction codes, which have been independently developed in France and in Spain. Such a bisite experience is particularly valuable for reducing the risk of incidental and nonsignificant observations.

At the numerical level, it appears that, even if they converge, NK techniques provide final results which are not really identical. The error on the result, measured by the residual difference on the scattered field, can be significantly reduced by means of an appropriate choice of the *a priori* information used to initiate the iterative process. The strategy in defining the regularization factor, as well as possible min/max constraints imposed on the reconstructed values of the dielectric constant, impact both the rate and the monotonous/oscillatory behavior of the convergence. Concerning experimental aspects, the knowledge of the temperature and dielectric constant of the external medium appears to have a very significant influence on the global accuracy of the dielectric constant distribution in the target, while the frequency affects more directly the Green's operators involved in the integral equation formulation. From a practical point of view, the control of the temperature in the whole water tank of the microwave scanner is probably more critical than the control of the frequency of the signal delivered by a microwave generator. More surprisingly, three facts merit to be pointed out. The first one is that a 20-dB dynamic range, or SNR, allows one to obtain satisfactory, even if perfectible, tomographic images. The well-known ill posedness of inverse problems could have led us to consider that much higher SNR should be required for proper reconstructions. On the contrary, the image quality is not drastically improved when the SNR is increased up to 40 dB. The second fact is that, for this particular scanner arrangement, free-space algorithms provide very good results, even for a closed-space equipment. Indeed, the measurement cell of the scanner is bounded by the circular array of antennas. The explanation is probably that, due to water immersion, the boundaries of the measurement cell of the scanner are not visible from the center of the cell, thanks to the high attenuation introduced by the water. This advantage adds to the previous ones recognized in the water immersion technique. The third fact is that pure two-dimensional reconstruction has provided satisfactory results, even with data collected by means of a three-dimensional experimental setup. Of course, such a difference between the reconstruction model and the experimental arrangement is responsible for a model error and, hence, degrades the effective SNR. As a matter of fact, this difference is partly compensated for via calibration procedures

conducted with a known target. A full compensation would require the sensors to be integrated in the reconstruction process.

Finally, the assessment of NK technique capabilities allows to consider different ways for improving and optimizing the performances of microwave scanners for a given application. First, the improvement of the dynamic range seems to be more efficiently achieved by reducing interferences and crosstalks between the different array elements, rather than by increasing the power. Second, the dielectric properties of the immersion medium could be optimized. The real part of the permittivity could be reduced, for improved penetration in living tissues, at the cost of larger wavelength. The imaginary part could also be reduced, at the cost of possible parasitic reflexions on the scanner boundaries. Similarly, reducing the frequency would simultaneously increase the SNR and make the boundaries more visible, requiring adequate formulation for compensating parasitic interactions between the target under test and the scanner. The number of sensors constitutes a factor of high practical relevance, for its impact on the cost, rapidity, and accuracy of the microwave scanner. The optimization of this sensor number cannot be conducted unless specifying the class of targets to be inspected, in terms of dielectric contrast, maximum dimension, heterogeneity, etc.

ACKNOWLEDGMENT

The cooperation between the French and the Spanish Groups has been undertaken within the Picasso Integrated Action Programs 1995/1996. The Spanish codes were run in vectorial computers operated by CEPBA (European Parallelism Center of Barcelona).

REFERENCES

- [1] J. Ch. Bolomey, Ch. Pichot, and G. Gaboriaud, "Planar microwave imaging camera for biomedical applications: Critical and prospective analysis of reconstruction algorithms," *Radio Sci.*, vol. 26, pp. 541–549, 1991.
- [2] A. Roger, "Newton–Kantorovich algorithm applied to an electromagnetic inverse problem," *IEEE Trans. Antennas Propagat.*, vol. AP-29, pp. 232–238, 1981.
- [3] W. C. Chew and Y. M. Wang, "Reconstruction of two-dimensional permittivity distribution using the distorted Born iterative method," *IEEE Trans. Med. Imag.*, vol. 9, pp. 218–225, 1990.
- [4] N. Joachimowicz, C. Pichot, and J. P. Hugonin, "Inverse scattering: An iterative numerical method for electromagnetic imaging," *IEEE Trans. Antennas Propagat.*, vol. AP-39, no. 12, pp. 1742–1752, 1991.
- [5] C. C. Chiu and Y.-W. Kiang, "Inverse scattering of a buried conducting cylinder," *Inverse Problems*, vol. 7, pp. 187–202, 1991.
- [6] R. E. Kleinman and P. M. Van den Berg, "A modified gradient method for two dimensional problems in tomography," *J. Comput. Appl. Math.*, vol. 42, pp. 17–35, 1992.
- [7] N. Joachimowicz, "Tomography microonde: Contribution à la reconstruction quantitative bidimensionnelle et tridimensionnelle," Ph.D. thesis, Univ. Paris VII, Gif-sur-Yvette, France, 1990.
- [8] J. J. Mallorqui, "Metodos numericos para aplicaciones biomedicas: Problemas directo e inverso electromagneticos," Ph.D. thesis, Univ. Politècnica de Catalunya, Catalunya, Spain, 1993.
- [9] A. Franchois, "Contribution à la tomography microonde: Algorithmes de reconstruction quantitative et vérifications expérimentales," Ph.D. thesis, Univ. Paris XI, Gif-sur-Yvette, France, 1993.
- [10] N. Joachimowicz, J. Ch. Bolomey, and Ch. Pichot, *ECAPT'93, 2nd Meeting of the BRITE-EURAM Concerted Action on Process Tomography*. Karlsruhe, Germany: Allemagne, 1993.
- [11] L. Jofre, M. S. Hawley, A. Broquetas, E. De Los Reyes, M. Ferrando, J. Romeu, and A. R. Elias-Fuste, "Medical imaging with a microwave tomographic scanner," *IEEE Trans. Biom. Imag.*, vol. 37, pp. 303–312, Mar. 1990.
- [12] A. Broquetas, J. Romeu, J. M. Rius, A. R. Elias-Fusté, A. Cardama, and L. Jofre, "Cylindrical geometry: A further step in active microwave tomography," *IEEE Trans. Microwave Theory Tech.*, vol. 39, pp. 836–844, May 1991.
- [13] J. H. Jacobi and L. E. Larsen, "Water immersed microwave antennas and their applications to microwave interrogation of biological targets," *IEEE Trans. Microwave Theory Tech.*, vol. MTT-27, pp. 70–78, Jan. 1979.
- [14] A. Stogryn, "Equations for calculating the dielectric constant of saline water," *IEEE Trans. Microwave Theory Tech.*, vol. MTT-19, pp. 733–736, 1971.
- [15] J. M. Rius, M. Ferrando *et al.*, "Microwave tomography: An algorithm for cylindrical geometries," *Electron. Lett.*, vol. 23, no. 11, pp. 564–565, May 1987.
- [16] J. M. Rius, Ch. Pichot, L. Jofre, J. Ch. Bolomey, N. Joachimowicz, A. Broquetas, and M. Ferrando, "Planar and cylindrical active temperature imaging," *IEEE Trans. Med. Imag.*, vol. 11, pp. 457–469, 1992.
- [17] G. H. Golub, M. Heath, and G. Wahba, "Generalized cross validation as a method for choosing a good ridge parameter," *Technometr.*, vol. 21, pp. 215–223, May 1979.
- [18] A. Franchois and Ch. Pichot, "Microwave imaging—Complex permittivity reconstruction with a Levenberg–Marquardt method," *IEEE Trans. Antennas Propagat.*, vol. 45, pp. 203–215, 1997.
- [19] J. J. Mallorqui, N. Joachimowicz, A. Broquetas, and J. Ch. Bolomey, "Quantitative images of large biological bodies in microwave tomography by using numerical and real data," *Electron. Lett.*, vol. 32, pp. 2138–2140, Nov. 7, 1996.
- [20] L. E. Larsen and J. H. Jacobi, "Microwaves offer promise as imaging modality," *Diagn. Imag., Clin. Med.*, vol. 11, pp. 44–47, 1982.
- [21] J. Ch. Bolomey and A. Joisel, "Microwave scanners for biomedical applications," in *Proc. Microwave and RF'95, Conf.*, London, Oct. 10–12, 1995, pp. 209–214.